Electrical Power Quality and Utilisation, Journal Vol. XIII, No. 2, 2007

The Use of the SSC as Reactive Power Compensator

Federico DELFINO and Renato PROCOPIO
University of Genoa, ITALY

Summary: **The paper deals with the possibility of employing the Custom Power Static Series Compensator (SSC), whose primary aim is to compensate voltage sags, also as a Reactive Power Compensator. The idea arises from the observation that such device does not work for the majority of time and can therefore be usefully employed for other purposes, such as power factor corrections. To this aim, an "ad hoc" control algorithm is developed and thoroughly discussed in the paper. The effectiveness of such control scheme is then tested by applying the SSC to a load represented by an induction motor in order to improve its power factor. The whole system is modelled with the aid of the electromagnetic code PSCAD-EMTDC, which allows to describe with high detail all its components. The results of the simulations show the good response of the device, which enables to rapidly increase the power factor of the motor and maintains the Total Harmonic Distortion (THD) of the injected phase voltages under the threshold value of 8%, as prescribed by CEI EN 50160 3.11.**

Key words:
power quality, custom power, DC-AC power conversion, reactive power, Static Series Compensator (SSC)

I. INTRODUCTION

In the second half of the 1990s, Power Quality has become a very important aspect of Power Delivery.

The increased interest of the scientific community towards this subject can be explained in a number of ways [1]. First of all, equipment has become more sensitive towards voltage disturbances and companies more sensitive to the deriving loss of production. On the other side, electronic equipment itself is responsible of 'bad Power Quality', since it can cause disturbances to other customers.

Moreover, the deregulated context of the electricity market has generated a growing need for standardization and performance criteria. In other words, since a customer can buy energy somewhere, the transport capacity somewhere else and pay the local utility for the connection to the grid, it is no longer clear who is the responsible for Power Quality and reliability.

It is also well worth noting that the increasing quality of the supply voltage has convinced customers that electricity 'must' always be present. As a consequence, a small deviation from ideal conditions is seen as a great problem.

All Power Quality phenomena, i.e. deviations of current or voltage from their ideal waveforms, can be divided into two main categories: variations and events.

The first ones occur when voltage or current is never equal to the ideal situation and so constant monitoring is required [1]. Among these kinds of disturbances, the most significant are variations in the magnitude and/or in the frequency. Another important phenomenon that belongs to the category of variations is the so-called current phase variation from the ideal condition, in which current and voltage are in phase, i.e. the power factor is equal to one, which enables the most efficient energy transport and the cheapest distribution system. Other variations are voltage unbalance and harmonic distortion in voltage or current waveform.

On the other hand, events are disturbances which occur only every once in a while. Probably the most significant example is the one relevant to interruptions in supply voltage. Typically, they are characterized by magnitude and duration. According to these parameters, one talks about voltage or supply interruptions or voltage dips or voltage sags, but more than one definition has been given [2–3], so it is not clear yet how to distinguish between the two categories. Other events are overvoltages caused by lightning strokes, switching operations or load reduction. Despite their short duration, all these events can disrupt an industrial process. So, the need of dedicated solutions for the mitigation of such events is great [4] and, since fast response is required, these technologies, commonly called Custom Power devices [5], are based on power electronics.

One of them, the Static Series Compensator (SSC), has been the subject of several investigations in the recent past [6–9]. Among these studies, in [9] the authors have proposed an effective control scheme for voltage sag compensation.

It should be underlined that, since a sag is typically characterized by a duration of some hundreds of milliseconds, such device could reasonably operate for few minutes in a year. In light of this fact, the idea of this paper is to suitably modify the SSC control system proposed in [9] to make it able to both compensate voltage sags and correct power factor when no sags occur. This would imply no extra costs for the reactive power compensation and give rise to a sort of "all in one" solution that could be appreciated by a customer who has to spend money for one device, which has two functions.

To test the efficiency of the new control system, the SSC has been connected in series to a medium voltage (MV) radial grid, feeding an induction motor. The whole system has been then implemented into the well-known PSCAD-EMTDC environment [10].

The paper is organized as follows: in section 2 a brief overview on the SSC structure is presented, and, next, in section 3, the SSC control scheme for the reactive power compensation is derived.

Then, in section 4, some numerical simulations are performed, whereas, in section 5, a detailed analysis on the SSC power factor correction capability is carried out.

Finally, in section 6, some conclusive remarks are drawn.

II. OVERVIEW ON THE SSC STRUCTURE

The complete SSC structure as well as some guidelines for the rating of its main components are described in detail in [9, 11, 12].

Basically, the SSC is connected in series between the supply network and the protected load, as shown in Figure 1, where:

— $v_1(t)$ is the supply grid phase voltage;
— $v_s(t)$ is the SSC series injection voltage;
— $v_2(t)$ is the load phase voltage;
— $i(t)$ is the load current.

As can be seen from Figure 1, the main components of a SSC are a DC-side energy source, a Voltage Source Converter (VSC) with an injection series transformer, a by-pass equipment, a disconnection equipment and an harmonic filter [9].

The DC-side energy source is necessary in order to provide a certain amount of the required load active power, when an event like voltage sag occurs. During the power factor correction such energy source has the only aim to compensate the IGBTs and the series transformer losses, since the SSC does not exchange any active power with the grid.

The converter employed in the SSC is a Voltage Source Converter (VSC) controlled by a Pulse Width Modulation (PWM) technique [13]. The most used VSC is the two-level converter, but a three-level converter can also be employed. In particular, the VSC under consideration in the present paper consists of a Neutral Point Clamped (NPC) three-level converter. It allows to continuously insert a voltage, which is identically equal to zero, by properly controlling the semi-conductor components. This means that, when no compensation is needed, there are no commutations and, as a consequence, no switching losses [14].

The most critical disturbances for the SSC are faults on the load side, that cause high current flows through the series transformer and the conducting VSC valves. Even if the turn-off devices are blocked, the fault current may circulate through the anti-parallel diodes. In order to prevent these devices from being thermally destroyed, a bypass equipment is used. This equipment consists of a bypass electronic switch, made up of two antiparallel thyristors, and a mechanical bypass switch, that allows the entire SSC to be bypassed (Fig. 1). When the feeder current becomes greater than a threshold level, the thyristors are triggered and start to conduct. Thyristors are suitable for this task, having a large short-time overload current capability and a low cost.

Finally, the passive filter is needed for blocking the high frequency harmonics generated by the PWM switching [15].

As far as the rating of these components is concerned [9], it should be underlined that it has been carried out keeping in mind the primary aim of the device, i.e. the use as voltage sag compensator. In the appendix, a careful analysis is carried out in order to show that the choice of the filters in [9] is also suitable for the present case, while, in section 5, some considerations are made on the influence of the rating of the DC voltage and of the series transformer on the SSC power factor correction capability.

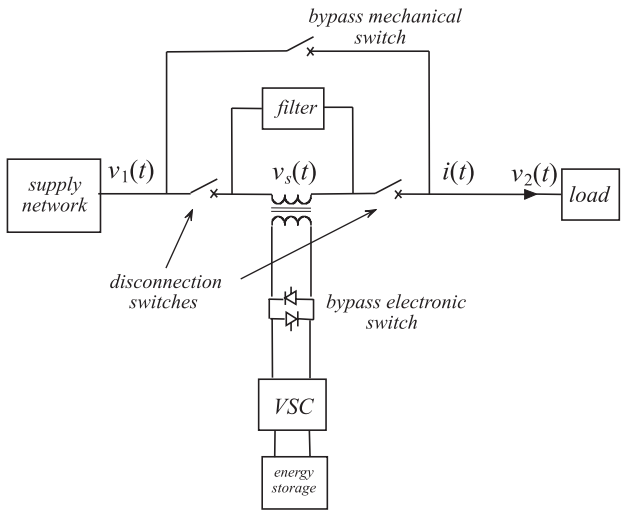

Fig. 1. SSC general structure

III. SSC CONTROL SCHEME FOR REACTIVE POWER COMPENSATION

Let us consider the situation depicted in Figure 2, where a SSC is placed in a MV radial grid to act as a reactive power compensator for a wound rotor induction motor.

It is important to highlight that the control scheme we are going to present is of general application. We chose to test it in the power factor correction of an induction motor because it represents a typical industrial application and it can be easily modelled in an electromagnetic code. Anyway, the choice of the load and, consequently, of its model, only influences the process of the regulator synthesis, but not the validity of the control scheme itself. Other typical loads that can be considered are the simple-impedance type load (Fig. 3) and the PQ type load (absorbing constant active and reactive power). As far as the first one is concerned, let us comment Figure 3, where there are two circuits with a grid represented by its Thevenin equivalent, and a load consisting of a resistance R and an inductance L. In the first circuit, the active and reactive power absorbed by the load are indicated as P' and Q'. Now let us insert a capacitor for the power factor correction (second circuit). Since the load is a simple-impedance type load, the absorbed active and reactive power

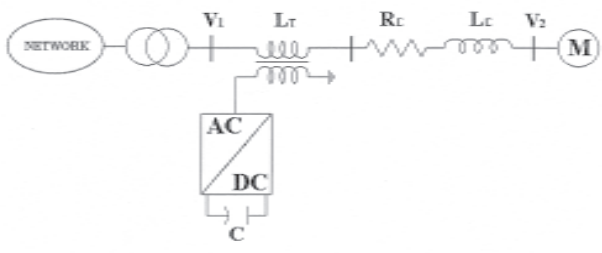

Fig. 2. Induction motor fed from a radial grid (R_C and L_C are, respectively, the resistance and the inductance of the cable connecting the motor to the SSC)

cannot be the same as before. Therefore, it is not possible to set up a power factor correction in its conventional form (i.e. without changing the load absorption).

In addition, the case of the PQ-load cannot be included in our analysis since such model has no meaning if implemented in an electromagnetic code like PSCAD-EMTDC. This code, taking into account electromagnetic transients, does not allow defining a constant PQ-load.

In the next subsection a suitable model of the induction motor is developed in order to set up an effective control algorithm.

A. Induction motor model

As well known, the induction motor can be described in the Laplace domain by the following set of equations, where all the variables are intended to be variations from steady-state conditions:

$$\begin{cases} \Delta V_{2d} = R_s \Delta i_d + s\Delta\varphi_{sd} - \omega\Delta\varphi_{sq} \\ \Delta V_{2q} = R_s \Delta i_q + s\Delta\varphi_{sq} + \omega\Delta\varphi_{sd} \end{cases} \quad (1)$$

$$\begin{cases} \Delta V'_{rd} = R'_r \Delta i'_{rd} + s\Delta\varphi_{sd} - \omega_r \Delta\varphi'_{rq} = 0 \\ \Delta V'_{rq} = R'_r \Delta i'_{rq} + s\Delta\varphi_{sq} + \omega_r \Delta\varphi'_{rd} = 0 \end{cases} \quad (2)$$

$$\begin{cases} \Delta\varphi_{sd} = (L_{s1} + L_m)\Delta i_d + L_m \Delta i'_{rd} \\ \Delta\varphi_{sq} = (L_{s1} + L_m)\Delta i_q + L_m \Delta i'_{rq} \end{cases} \quad (3)$$

and:

$$\begin{cases} \Delta\varphi'_{rd} = (L'_{r1} + L_m)\Delta\ \ i'_{rd} + L_m \Delta i_d \\ \Delta\varphi'_{rq} = (L'_{r1} + L_m)\Delta i'_{rq} + L_m \Delta i_q \end{cases} \quad (4)$$

where, referring to Figure 2:

— $\Delta V_{2d(q)}$ is the stator direct (quadrature) axis voltage
— $\Delta V'_{rd(q)}$ is the rotor direct (quadrature) axis voltage
— $\Delta i_{d(q)}$ is the stator direct (quadrature) axis current
— $\Delta i'_{rd(q)}$ is the rotor direct (quadrature) axis current
— $\Delta\varphi_{sd(q)}$ is the stator direct (quadrature) axis flux
— $\Delta\varphi'_{rd(q)}$ is the rotor direct (quadrature) axis flux
— $R_{s(r)}$ is the stator (rotor) resistance
— $L_{s(r)1}$ is the stator (rotor) leakage inductance
— L_m is the magnetizing inductance
— ω and ω_r are the angular frequency and the slip factor.

The symbol ' has been added to the quantities referred to the stator.

If one puts (4) and (3) into (2), it readily follows that:

$$\begin{cases} \Delta i'_{rd} = -\alpha(s)\Delta i_d + \beta(s)\Delta i_q \\ \Delta i'_{rq} = -\beta(s)\Delta i_d - \alpha(s)\Delta i_q \end{cases} \quad (5)$$

being respectively:

$$\alpha(s) = \frac{L_m\left[sR_r + (s^2 + \omega_r^2)L_r\right]}{(R_r + sL_r)^2 + \omega_r^2 L_r^2} \quad (6)$$

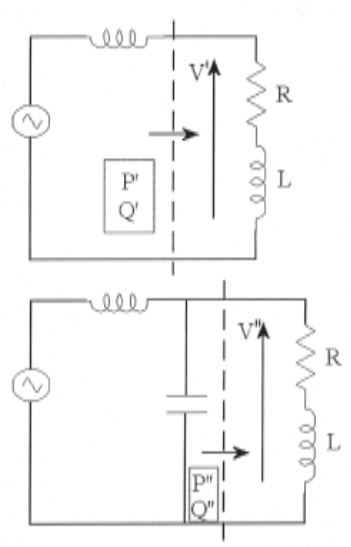

Fig. 3. Simple-impedance type load

and:

$$\beta(s) = \frac{R_r \omega_r L_m}{(R_r + sL_r)^2 + \omega_r^2 L_r^2} \quad (7)$$

and having posed $L_r = L_m + L_{r1}$.
Now inserting (5) into (3), one has:

$$\begin{cases} \Delta\varphi_{sd} = \left[L_s - \alpha(s)L_m\right]\Delta i_d + \beta(s)L_m \Delta i_q \\ \Delta\varphi_{sq} = -\beta(s)L_m \Delta i_d + \left[L_s - \alpha(s)L_m\right]\Delta i_q \end{cases} \quad (8)$$

having defined L_s as $L_s = L_m + L_{s1}$. Finally, introducing the above expressions for the stator fluxes into (1), one gets the following relationship between stator currents and voltages:

$$\Delta V_{2d} = \left[\left(R_s + \omega\beta(s)L_m\right) + s\left(L_s - \alpha(s)L_m\right)\right]\Delta i_d - \\ -\left[s\beta(s)L_m - \omega\left(L_s - \alpha(s)L_m\right)\right]\Delta i_q \quad (9)$$

and:

$$\Delta V_{2q} = \left[\left(R_s + \omega\beta(s)L_m\right) + s\left(L_s - \alpha(s)L_m\right)\right]\Delta i_q + \\ +\left[s\beta(s)L_m - \omega\left(L_s - \alpha(s)L_m\right)\right]\Delta i_d \quad (10)$$

As can be noticed from equations (9 and 10), the induction motor model is characterized by two dynamic relationships, which could make it difficult to perform the control system synthesis. In order to overcome such problem, one can simplify equations (9 and 10) by neglecting the slip factor ω_r. However, such assumption, which is reasonable at steady state conditions, will be used only to set the numerical values

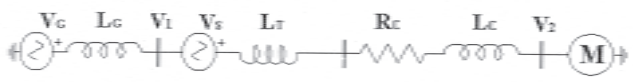

Fig. 4. System model for the control algorithm setup

of the regulator parameters, while the complete model (as built-in in the PSCAD environment) will be chosen to perform the numerical simulations.

Setting $\omega_r = 0$, one has:

$$\begin{cases} \Delta V_{2d} = a(s)\Delta i_d - \omega b(s)\Delta i_q \\ \Delta V_{2q} = \omega b(s)\Delta i_d + a(s)\Delta i_q \end{cases} \tag{11}$$

being respectively:

$$a(s) = \frac{R_r R_s + s\left(L_r R_s + L_s R_r\right) + s^2\left(L_s L_r - L_m^2\right)}{\left(R_r + sL_r\right)} \tag{12a}$$

and:

$$b(s) = \frac{L_s R_r + s(L_r L_s - L_m^2)}{(\mathrm{R}_r + s\,\mathrm{L}_r)} \tag{12b}$$

B. Control algorithm

Let us consider Figure 4, where the network is represented by its Thevenin equivalent (being V_G the voltage and L_G the inductance), the SSC by a voltage source V_S in series with the transformer leakage inductance L_T and the cable connecting the SSC to the motor by the series $R_c - L_c$.

Recalling (11), one easily gets:

$$\Delta V_{1d} + \Delta V_{sd} - (a(s) + sL + R)\Delta \mathrm{i_d} + \left[\omega(L + b(s))\right]\Delta i_\mathrm{q} = 0 \tag{13}$$

and:

$$\Delta V_{1q} + \Delta V_{sq} - (a(s) + sL + R)\Delta \mathrm{i_q} - \left[\omega(L + b(s))\right]\Delta i_\mathrm{d} = 0 \tag{14}$$

being $L = L_c + L_t$ an $R = R_c$.

Equations (13 and 14) represent the system model whose controlled variables are the series injected voltages ΔV_{sd} and ΔV_{sq}, while the disturbances are the grid voltages ΔV_{1d} and ΔV_{1q} and the regulated variables are the current $\Delta \mathrm{i_d}$ and Δi_q.

As a matter of fact, it can be observed that, choosing the initial angle of the Park transformation in such a way that $V_{1q} = 0$, it readily follows that [13]:

$$\begin{cases} p = V_{1d} i_d \\ q = -V_{1d} i_q \end{cases} \tag{15}$$

being p and q the active and reactive power at grid level. As a consequence, one can evaluate the power factor cosφ as:

$$\cos\varphi = \frac{i_d}{\sqrt{i_d^2 + i_q^2}} \tag{16}$$

Now, if one is able to control the following ratio:

$$k = tg\varphi = \frac{i_q}{i_d} \tag{17}$$

it is then possible to reach the goal of improving the power factor.

It should be stressed that it is not necessary to control both the direct axis current and the quadrature axis one, but only their ratio. This means that another degree of freedom is present, which can be used imposing that the active power exchanged between the SSC and the system is zero, that is to say:

$$V_{sd} i_d + V_{sq} i_q = 0 \tag{18}$$

Thus, recalling (17 and 18), it follows that the two Park components of the injected voltage are not independent, but the following relationship must hold:

$$\Delta V_{sd} = -k\Delta V_{sq} \tag{19}$$

Finally, indicating with:

$$\Delta x_q = \Delta V_{sq} - \left\{ \omega\left[L + b(s)\right] \right\}\Delta i_d + \Delta V_{1q} \tag{20}$$

the output of the regulator block, the resulting control scheme is the one depicted in Figure 5, while the resulting control loop is the one sketched in Figure 6. The control scheme requires the measurement and the Park transforms of both the current absorbed by the motor and the network voltage. As can be seen from Figure 5, the control algorithm includes a dynamic compensation, whose parameters come out from measurements. In our analysis, we did not consider the parameter uncertainties, which can be taken into account by means of a sensitive analysis in a further development of this research work.

C. Regulator synthesis

The process transfer function G has the following form:

$$G(s) = \frac{1}{R + sL + a(s)} = \frac{n_0 + n_1 s}{d_0 + d_1 s + d_2 s^2} \tag{21}$$

where the meaning of the symbols is the following:

— $n_0 = \mathrm{R}_r$
— $n_1 = \mathrm{L}_r$
— $d_0 = \mathrm{R}_r\mathrm{R}_s + \mathrm{R}\mathrm{R}_r$
— $d_1 = \mathrm{R}_s\mathrm{L}_r + \mathrm{L}_s\mathrm{R}_r + \mathrm{L}_r\mathrm{R} + \mathrm{L}\mathrm{R}_r$
— $d_2 = \mathrm{L}_s\mathrm{L} + \mathrm{L}_s\mathrm{L}_r - \mathrm{L}_m^2$

Choosing an integral regulator:

$$\mathrm{R}_q(s) = \frac{\mathrm{K}_I}{s} \tag{22}$$

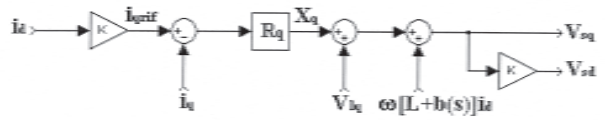

Fig. 5. Control algorithm for the power factor correction

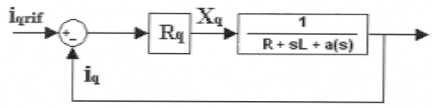

Fig. 6. Control loop for the power factor correction

after simple algebraic manipulations, one obtains that the closed loop transfer function $G_c(s)$ has the following form:

$$G_c(s) = \frac{K_I n_0 s + K_I n_1 s^2}{(K_I n_1 + d_2)s^2 + (K_I n_0 + d_1)s + d_0} \tag{23}$$

and the poles are:

$$s_{1,2} = \frac{-(K_I n_0 + d_1) \pm \sqrt{(K_I n_0 + d_1)^2 - 4d_0(K_I n_1 + d_2)}}{2(K_I n_1 + d_2)} \tag{24}$$

In order to ensure stability, recalling the expressions for n_0, n_1 and d_1, one must set:

$$K_I > \frac{L_m^2 - L_R L - L_S L_R}{L_R} \tag{25}$$

Equation (25) implies that, according to our model, the regulator gain can increase indefinitely without creating stability problems. Of course, this is due to the approximations of our mathematical model, since for gains approaching infinity no doubt the system will become unstable.

IV. NUMERICAL RESULTS

In the following some numerical results are presented and discussed in order to show the effectiveness of the developed control scheme. The main numerical data are summarized in Table 1.

As a test case, we have considered the situation in which an induction motor starts without any mechanical load; after 1.2 seconds its rated mechanical torque is applied, and after another transient of about 0.8 s, the machine reaches its steady state conditions, with power factor 0.85. Then, at $t = 5$ s, the control system is applied in order to increase $\cos\varphi$ to 0.9.

In Figure 7, it is shown that the power factor increases from about 0.85 to 0.9, while the absolute value of the ratio k (which is negative, being the motor an inductive load) defined in (17) decreases to 0.5 (see Fig. 8).

The active and reactive powers at the grid bus, defined in (15), have been plotted in Figures 9 and 10 respectively. As can be seen, the active power does not vary significantly,

Table 1. Main parameters of the test case.

Supply network	Rated voltage	15 kV
	Short circuit power	100 MVA
	Frequency	50 Hz
Series transformer	Rated power	0.6 MVA
	Primary rated voltage	4.33 kV
	Secondary rated voltage	1.33 kV
	Short circuit voltage	5%
	Winding connection	Yy
Voltage source converter	DC-side rated voltage	4 kV
	Frequency modulation ratio	mf=78
Harmonic filter	Filter resistance	1 Ω
	Filter capacitance	500 μF
Step down transformer	Rated power	1.2 MVA
	Primary rated voltage	15 kV
	Secondary rated voltage	6.1 kV
	Short circuit voltage	5%
	Winding connection	Yy
Induction motor data	Rated power	1.087 MVA
	Rated voltage	6 kV
	Rated current	105 A
	Frequency	50 Hz
	Angular moment of inertia (Ta=2H)	0.47 s
Induction motor: equivalent circuit parameters	Stator resistance	0.015 p.u.
	Rotor resistance	0.1 p.u.
	Stator leakage inductance	0.2 p.u.
	Rotor leakage inductance	0.2 p.u.
	Magnetizing inductance	3.5 p.u.
Cable	Resistance	30 mΩ
	Inductance	0.06 mH
DC Capacitor	Capacitance	52 mF
Regulator	Gain	100

while the reactive one decreases, as requested by the control algorithm.

The active and reactive powers of the motor defined as:

$$\begin{cases} p_m = V_{2d} i_d + V_{2q} i_q \\ q_m = -V_{2d} i_q + V_{2q} i_d \end{cases} \tag{31}$$

are plotted in Figures 11 and 12. As can be seen, there are no significant variations due to the compensation action; this confirms the fact that, for simple applications, the induction motor operating at steady state conditions can be considered as a constant power load.

Figures 13 and 14 the mechanical speed and the motor torque (in p.u. on motor basis) are plotted. As can be noticed, there is a slight variation on the speed, from 0.895 p.u. to 0.91 p.u.

As far as the voltages are concerned, it can be noted that the network one does not vary (Fig. 15), while the load one grows up from 5.8 kV to 6.2 kV, being the rated one 6 kV (Fig. 16).

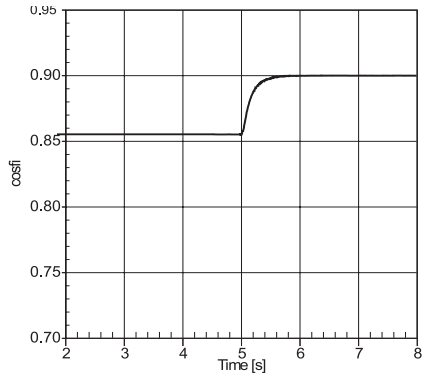

Fig. 7. Improvement of the power factor

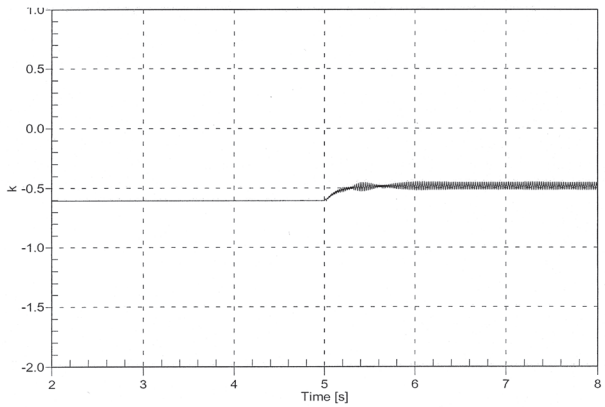

Fig. 8. Variation of the ratio $k=i_q/i_d$

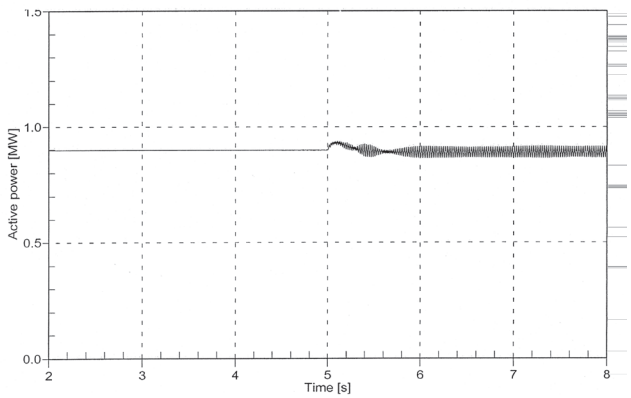

Fig. 9. Active power at the grid bus

Such deviation seems to be acceptable, being 200/6000 = 3.3%, which is lower than 5% [2].

In Figure 17, the injected phase voltages are plotted. We can observe that the PWM harmonics are attenuated by the passive filters; we have also verified that the Total Harmonic Distortion (THD) is lower than 8%, as prescribed by CEI EN 50160 3.11 [2].

Finally, Fig. 18 shows that the DC side voltage does not decrease substantially. Actually, due to constraint (18), it should be constant. But the DC capacitor has to compensate the IGBT losses, as well as the resistance filter ones and this means that, for compensations of higher entity, (18) is not sufficient to prevent the DC capacitor from discharging and so another control loop should be implemented in order to keep the DC voltage sufficiently near to its rated value.

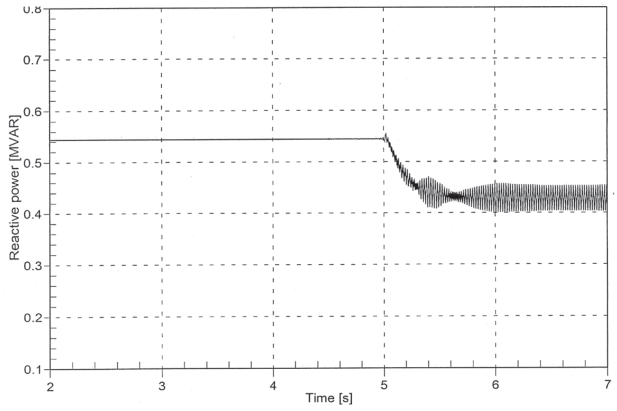

Fig. 10. Reactive power at the grid bus

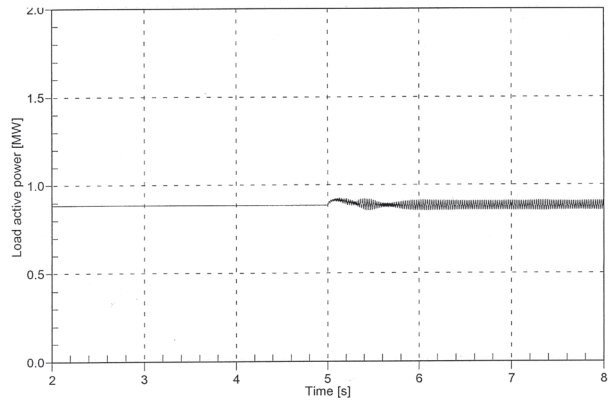

Fig. 11. Active power at the motor bus

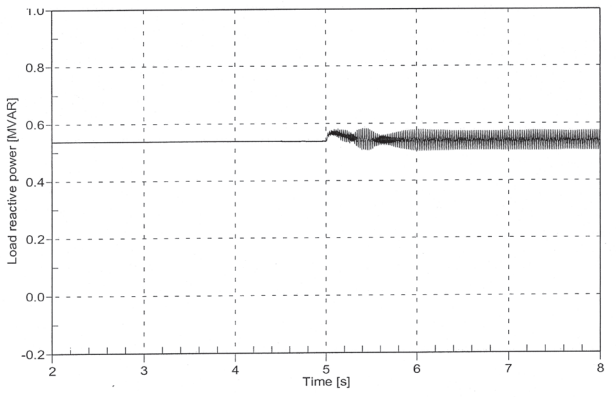

Fig. 12. Reactive power at the motor bus

V. POWER FACTOR CORRECTION CAPABILITY

As mentioned in section II, the SSC rating has been chosen in order to compensate voltage sags [6]. In this section, a simple analysis will be carried out to demonstrate how such choice affects the SSC power factor correction capability.

Let us reconsider (9 and 10); combining them with Kirchhoff Voltage Law (KVL) applied to circuit of Figure 4, at steady state conditions [13] one has:

$$V_{1d} + V_{sd} = c_d i_d - c_q \quad i_q \tag{32}$$

and:

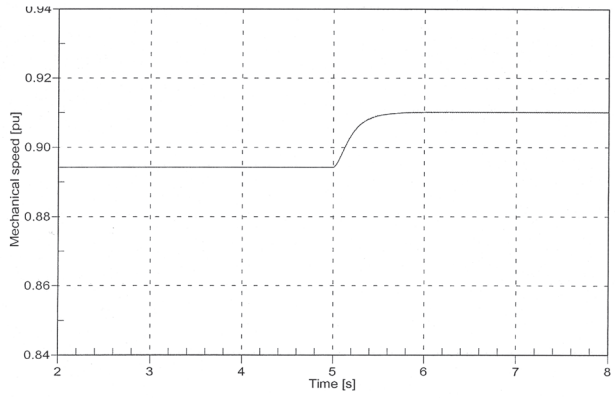

Fig. 13. Mechanical speed

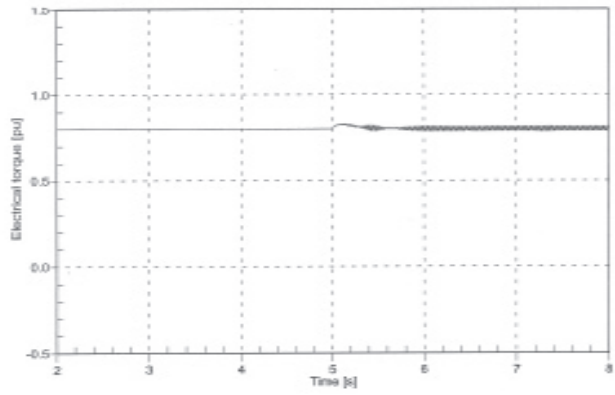

Fig. 14. Motor torque

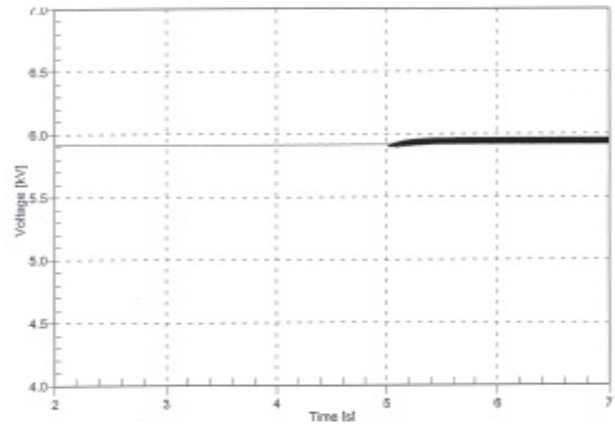

Fig. 15. RMS value of the network line-to-line voltage

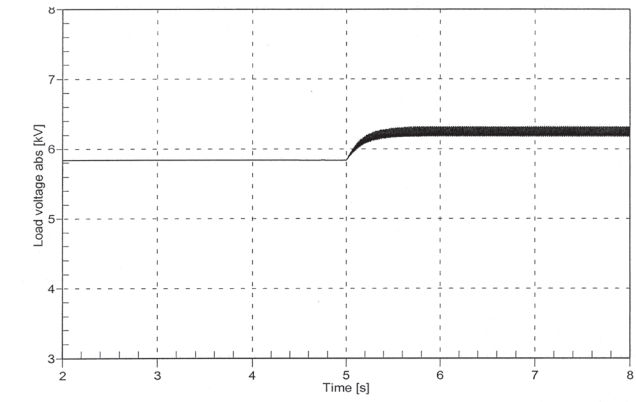

Fig. 16. RMS value of the motor line-to-line voltage

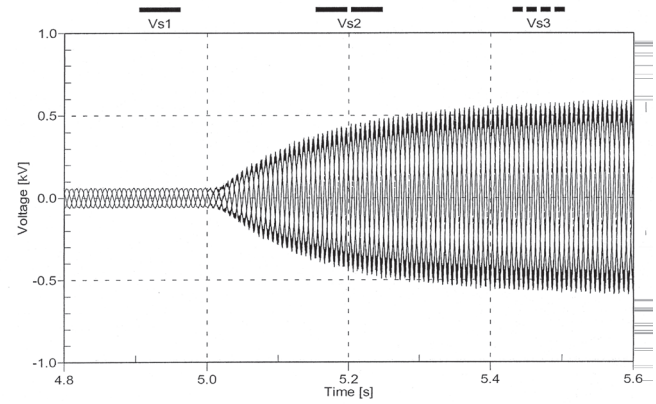

Fig. 17. Injected phase voltages

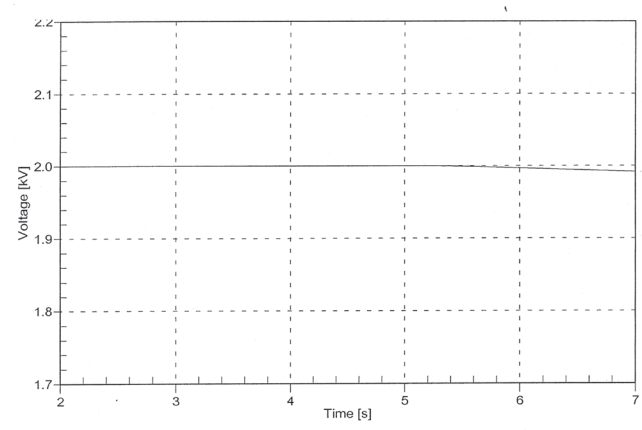

Fig. 18. DC side voltage

$$V_{1q} + V_{sq} = c_d i_q + c_q i_d \tag{33}$$

being:

$$c_d = R + R_S + \omega\beta(0) L_m \tag{34}$$

and:

$$c_q = L + L_S - \alpha(0) L_m \tag{35}$$

Equations (32 and 33), for assigned V_{1d} and V_{1q} (in our case $V_{1q} = 0$, as mentioned in section 3), form a system of two equations and four unknowns, namely i_d, i_q, V_{sd} and V_{sd}.

Recalling now (17 and 19), one easily gets the two missing equations necessary to solve the system, i.e.:

$$i_d = \frac{V_{1d}}{c_d\left(1+k^2\right)} \quad \text{and} \quad i_q = \frac{kV_{1d}}{c_d\left(1+k^2\right)} \tag{36}$$

and:

$$V_{sq} = \frac{\left(kc_d + c_q\right)V_{1d}}{c_d\left(1+k^2\right)} \quad \text{and} \quad V_{sd} = \frac{-k\left(kc_d + c_q\right)V_{1d}}{c_d\left(1+k^2\right)} \tag{37}$$

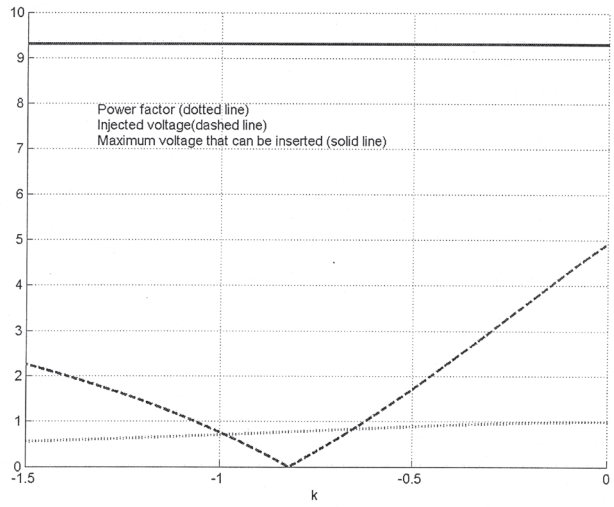

Fig. 19. SSC compensation capability: power factor, injected voltage and maximum limit for the SSC voltage

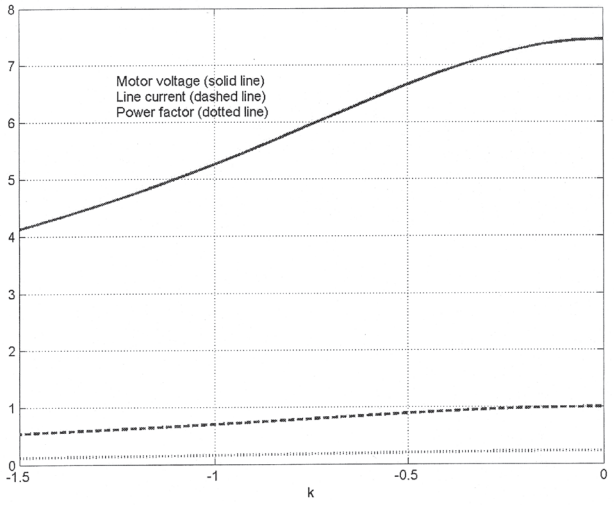

Fig. 20. SSC compensation capability: power factor, motor voltage and current

Equations (36 and 37) express the *d-q* axis motor current and the *d-q* axis voltages the VSC has to inject to obtain the desired power factor (i.e. for an assigned *k*). Finally, the amplitude of such current and voltage are given by:

$$I^2 = \frac{{V_{1d}}^2}{{c_d}^2\left(1+k^2\right)} \tag{38}$$

$${V^2}_s = \frac{\left(kc_d + c_q\right)^2 {V_{1d}}^2}{{c_d}^2\left(1+k^2\right)} \tag{39}$$

In Figure 19, the power factor $\cos\varphi = \frac{1}{1+k^2}$, the injected voltage V_s and the maximum voltage that can be inserted [9] have been plotted as a function of k, while in Figure 20 the power factor appears together with the RMS value of the current and of the motor voltage. This latter has been calculated applying again KVL to circuit of Figure 4.

As can be seen from Figure 19, the maximum voltage that can be inserted is higher than the required voltage to obtain power factor equal to one, so from this point of view the system seems to be effective. But since the motor voltage grows up more rapidly than cosφ (see Fig. 20), the overvoltage protection tripping could occur 'before' the full compensation of the reactive power. This means that, in some cases, only small compensations are possible.

VI. CONCLUSIONS AND PERSPECTIVES OF FUTURE WORK

In this paper the use of the SSC as reactive power compensator has been analyzed and discussed.

An effective control algorithm has been developed and implemented in order to reach the power factor correction.

Such control scheme has been tested in a real situation, namely the improvement of the power factor of an induction motor fed from a MV radial grid. The whole system has been modeled with the aid of the electromagnetic code PSCAD-EMTDC, which allows to describe all the components with high detail.

Future activity will concern the possibility of applying the algorithm in more complex situations, such as many induction motors fed from a bus connected to a SSC or a motor provided with an automatic speed control loop.

Finally, if the system requires compensation of higher entity, it will be necessary to implement a control loop also able to keep the DC side voltage constant.

VII. APPENDIX – THE HARMONIC FILTER

Let us consider the circuit of Figure 21, where the SSC is represented by an ideal voltage source $K_t V_{ch}$, being h the generic harmonic order.

Since the motor equations are given in the Park domain, all the analysis will be carried out considering for all the phase variables (x_a, x_b, x_c) the corresponding Park space vector $\bar{x} = x_d - jx_q$.

As a consequence, in the frequency domain, one has:

$$\begin{cases} \bar{V}_{sh} = \bar{E}_{gh} - jh\omega L_s \bar{i}_{1h} + j\omega L_s \bar{i}_{1h} - R_c \bar{i}_{1h} - a(jh\omega)\bar{i}_{1h} - j\omega b(jh\omega)\bar{i}_{1h}, \\ \bar{V}_{sh} = -k\bar{V}_{ch} - jh\omega L_t \bar{i}_{3h} + j\omega L_t \bar{i}_{3h}, \\ \bar{V}_{sh} = -R_f \bar{i}_{2h} - \frac{jh\omega}{C_f(1-h^2)\omega^2}\bar{i}_{2h} - j\frac{\omega}{C_f(1-h^2)\omega^2}\bar{i}_{2h}, \end{cases} \tag{A1}$$

being $L_s = L_c + L_g$.

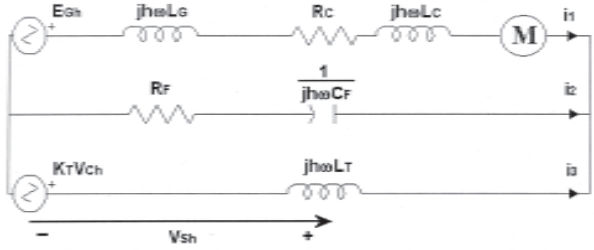

Fig. 21. Equivalent circuit for the harmonic filter design

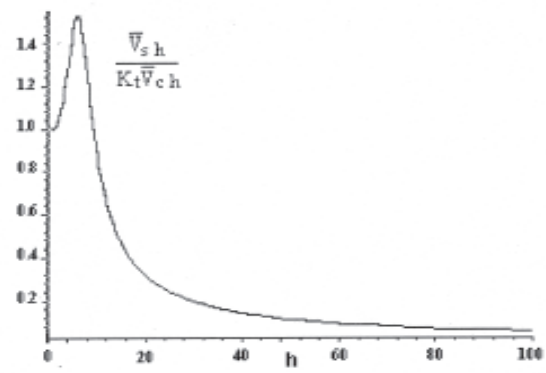

Fig. 22. Harmonic filter response

Now applying the Millmann theorem to the circuit sketched in Figure 21, one has:

$$\bar{V}_{s,h} = \frac{\dfrac{\bar{E}_{g,h}}{Z_1} + \dfrac{K_t \bar{V}_{c,h}}{Z_2}}{\dfrac{1}{Z_1} + \dfrac{1}{Z_2} + \dfrac{1}{Z_3}} \qquad \text{(A2)}$$

being, respectively:

$$Z_1 = R_C + j(h-1)\omega L_s + a(jh\omega) - j\omega b(jh\omega) \qquad \text{(A3)}$$

$$Z_2 = j(h-1)\omega L_t \qquad \text{(A4)}$$

and:

$$Z_3 = R_F + \frac{1}{j(h-1)C_F\omega} \qquad \text{(A5)}$$

Now, imposing that, for the minimum harmonic order $h_{\min}$, it must hold true that $\dfrac{\bar{V}_{s,h}}{K_t \bar{V}_{c,h}} << 1$ and, for the fundamental frequency (h = 1), one should have $\dfrac{\bar{V}_{s,h}}{K_t \bar{V}_{c,h}} \cong 1$, one can obtain the values for R_f and C_f.

In Figure 22, the filter response is plotted as a function of the harmonic order h (R_f= 1 W and C_f= 500 mF). As can be noticed the existing harmonic orders, approximately near $h = m_f = 78$, are properly attenuated.

REFERENCES

1. Bollen M.H.J.: *Understanding Power Quality Problems: Voltage Sags and Interruptions*, New York, IEEE Press, 1999.
2. European Standard EN 50160. *Voltage characteristics of electricity supplied by public distribution systems*. CENELEC, 1999.
3. IEEE Std. 1159–1995: *Recommended Practice on Monitoring Electric Power Quality*. 1995.
4. CIGRE Working Group 37.28. *Quality of Supply – Customers Requirements*. June 2001
5. Hingorani N.G.: *Introducing Custom Power*. IEEE Spectrum, June 1995, pp. 41–48.
6. Sannino A. and Svensson J.: *A series-connected voltage source converter for voltage sag mitigation using vector control and a filter compensation algorithm*. Proc. IEEE Industry Applications Society Annual Meeting, Roma, Italy, October 2000.
7. De Oliveira M.M.: *Power electronics for mitigation of voltage sags and improved control of AC power systems.* Doctoral Dissertation, The Royal Institute of Technology, Stockholm, Sweden, 2000.
8. Nielsen J.G., Blaabjerg F. and Mohan N.: *Control strategies for dynamic voltage restorer compensating voltage sags with phase jump*. Proc. Applied Power Electronics Conf. Expo., vol. 2, 2001, pp. 1267–1273.
9. Delfino B., Fornari F., Procopio R.: *An Effective SSC Control Scheme for Voltage Sag*. IEEE Trans. on Power Delivery, vol. 20, n. 3, July 2005, pp. 2100–2107.
10. PSCAD-EMTDC version 3.0, The Professional's Tool for Electromagnetic Transients Simulation, Manitoba HVDC Research Centre Inc., 2001.
11. Daehler P., Eichler M., Gaupp O., Linhofer G.: *Power Quality devices improve manufacturing process stability*. ABB Review, 1/2001, pp. 32–42.
12. Jauch T., Kara A., Rahmani M., Westermann D.: *Power Quality ensured by dynamic voltage correction*. *ABB Review*, 4/1998, pp. 25–35.
13. Mohan N., Undeland T.M., Robbins W.P.: *Power Electronics*. John Wiley & Sons, 1995.
14. Daehler P., Affolter R.: *Requirements and solutions for Dynamic Voltage Restorer, a case study*. Proceedings of IEEE Power Engineering Society Winter Meeting 2000, vol. 4, pp. 2864–2871.
15. Choi S.S., Li B.H., Vilathgamuwa D.M.: *Design and Analysis of the Inverter-Side Filter Used in the Dynamic Voltage Restorer*. IEEE Trans. on Power Delivery, vol. 17, No. 3, July 2002, pp. 857–864.
16. Schauder C., Mehta H.: *Vector Analysis and Control of Advanced Static VAR Compensators*. IEE Proceedings-C, vol. 140, No. 4, July 1993, pp. 299–306.

Federico Delfino
was born in Savona, Italy, on February 28th, 1972. He graduated cum laude in Electrical Engineering from the University of Genoa, in 1997 and received the PhD degree from the same University in 2001. He is currently a Researcher at the Department of Electrical Engineering of the University of Genoa. His research interests are mainly focused on electromagnetic compatibility, especially on transmission line modeling and power quality improvement in distribution networks. He is the author or coauthor of more than 60 scientific papers presented at international conferences and published in reviewed journals. Dr. Delfino is a member of the IEEE and of the Italian Electrical Engineering Association (AEIT).
Correspondence address:
Department of Electrical Engineering, University of Genoa,
Via Opera Pia 11a, I-16145 Genova, ITALY
Tel.: +39 010 353 2721, Fax: +39 010 353 2700
e-mail: federico.delfino@die.unige.it

Renato Procopio
was born in Savona, Italy, on March 6th, 1974. He graduated cum laude in Electrical Engineering from the University of Genoa in 1999 and received the PhD degree from the same University in 2004. He is currently a Researcher at the Department of Electrical Engineering of the University of Genoa. He works on lightning return stroke current modeling and TL theory as well as on power quality improvement in distribution networks. He is the author or coauthor of more than 50 scientific papers presented at international conferences and published in reviewed journals. Dr. Procopio is a member of the IEEE and of the Italian Electrical Engineering Association (AEIT).
Correspondence address:
Department of Electrical Engineering, University of Genoa,
Via Opera Pia 11a, I-16145 Genova, ITALY
Tel. +39 010 353 2730, Fax +39 010 353 2700
e-mail: procopio@die.unige.it